

# The Applicability of Pulsed Plasma Thrusters to Rendezvous and Docking of Cubesats

IEPC-2013-424

*Presented at the 33<sup>rd</sup> International Electric Propulsion Conference,  
The George Washington University, Washington, D.C., USA  
October 6–10, 2013*

Stephen Gabriel and Eric Rogers\*  
*University of Southampton, England*

Mirko Leomanni†  
*University of Siena, Italy*

Despite the interest in formation flying and cubesats over something like the last decade or so, close controlled formation flying of two cubesat size spacecraft has not been achieved. Similarly, despite the growing interest in propulsion systems for cubesats, there are very few commercially available and flight ready systems. If these are coupled with the realization that formation flying could be an enabling technology for cubesats [1] enhancing capabilities and opening up possibilities for new types of missions, it seemed timely to revisit the problem of rendezvous and docking for cubesats to examine what might be possible with a pulsed propulsion system based on a pulsed plasma thruster (PPT) that is close to flight qualification [2].

The approach taken was to build on previous work [3,4] which developed a universal adaptive control system for formation flying by adding constraints on the actuators in terms of their pulsed nature and also actual performance characteristics. The formalism and theory to solve this problem has been achieved but due to numerical problems in solving the equations, there are no results as yet. However, another simpler approach has been applied and some preliminary results are presented.

## I. Introduction

Future applications of cubesats, such as drag make-up, de-orbit, plane changes, formation flying and rendezvous and docking, will require a propulsion subsystem [1]. Because of the severe volume, power and mass requirements imposed on even a 3U configuration, the performance and lifetime of the propulsion subsystem are challenging. Several possible options exist, including cold gas, micro-resistojet, micro-colloid, VATs and pulsed plasma thrusters (PPTs). But in terms of flight readiness, few systems are currently available.

The paper addresses the suitability of a miniaturized PPT, called PPTCUP [2], which is very close to being flight qualified, having recently completed 1 million shots in a life testing campaign. Using a set of typical requirements for orbit control for a cubesat mission that would involve both formation flying the ability of a cluster of these thrusters is investigated from a control perspective ie can the thrusters meet all the control requirements given the constraints not only on controllability but mass, volume, power, number of thrusters and their location.

The control systems used in small spacecraft lead to a possible conflict between the control signals required by the model to achieve the performance objectives and the safe operating ranges of the actuators. In such cases, a constrained control design is required, where both input and output constraints will be required.

---

\*Electronics and Computer Science, sbg2@soton.ac.uk.

†Dipartimento di Ingegneria dell'Informazione e Scienze matematiche, leomanni@dii.unisi.it.

One option is to use model predictive control, based on computing the optimal controls over a finite number of future sampling instances under a receding horizon strategy.

Modeling the future control trajectory is a critical task. The traditional approach is to embed an integrator in the design and the incremental control trajectory is then directly computed within an optimization window. The main drawback is the requirement to optimize a large number of parameters if fast sampling is required and/or the system has a relatively complex dynamic response.

Fast sampling is typically required for mechanical and electro-mechanical systems because the time constants arising in the various sub-components can vary in duration and a smaller sampling interval is required to capture the effects of the smaller of these. One approach [3] to reduce the number of parameters requiring optimization on-line is to parameterize the future trajectory of the filtered control signal using a set of Laguerre functions, where a scaling factor is used to reflect the time scale of the predictive control system.

This setting extends naturally to include, with particular relevance to the application area in this paper, input amplitude. The control design problem then is to minimize a cost function subject to linear inequality constraints. This approach to design poses three major challenges when the solution uses quadratic programming, the first of which is the lack of a guarantee for the existence of a constrained optimal solution. For example, if both the input and output constraints are violated they will be in conflict and the quadratic programming solution becomes infeasible. Secondly, since the solution is computed in real-time and involves an iterative computation, the algorithms used must be sufficiently fast to enable computation within one sampling period. This is one of the main reasons why model predictive control finds many applications in process control where the sampling period can be of the order of minutes. In contrast, for electro-mechanical systems such as the robotic system considered in this paper, the sampling period is much less than a second. Thirdly, as for all other engineering applications, there must be safety protection mechanisms in place to ensure stability of the controlled system in the event that the quadratic programming algorithm fails to reach a constrained optimal solution. The quadratic programming algorithm used in this paper has features suitable for real-time computation of this constrained optimal problem in terms of these challenges.

This paper will give the underlying theory of a detailed simulation-based assessment of the performance achievable under this design as applied to the problem of formation flying of cubesat size spacecraft. The approach can be extended to the control of rendezvous and docking of similar size spacecraft which will include attitude as well as orbit control.

## II. The thruster

The PPT thruster chosen is the PPTCUP developed by Mars Space Ltd, Clyde Space Ltd and the University of Southampton [5]. This thruster is a side-fed ablative PPT using Teflon as propellant and has been specifically designed for application to cubesats. A 3-D schematic of the thruster is shown in Figure 1. The design of this thruster, which is an EM model, incorporates some significant changes from the baseline PPTCUP breadboard( designated PPTCUP-BB and developed and tested in 2011(42,58sctransfer)) to not only meet the stringent mass, volume and power constraints for cubesat applications but to meet lifetime and flight qualification requirements. Two particular problems have been solved to meet the lifetime of 1 million

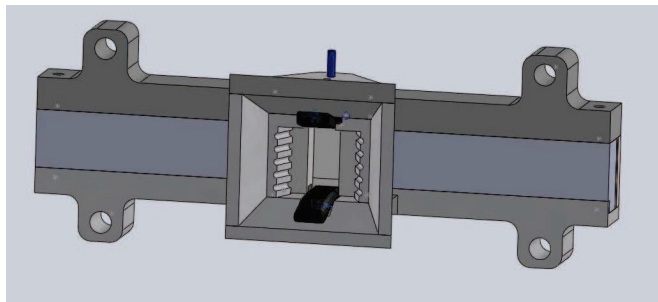


Figure 1. 3-D diagram of the PPTCUP Engineering Model.

shots, carbonization of the back plate and spark plug lifetime. As can be seen from Figure 1 a series of lateral grooves on the sidewalls have been introduced to prevent electrode shorting and not visible in Figure

1 but equally important a second back plate or shield to protect the back-plate from deposits of carbon. To increase the spark plug longevity, changes have been made in the propellant or insulating material across which the spark is discharged. In addition the electrode shape has been changed for performance reasons and since the nozzle divergence angle has remained the same this has the added benefit of creating a gap between the electrodes and sidewalls which also helps prevent shorting due to carbonisation. Other changes have been made to the materials used for manufacturing [5]. Table 1 shows the key characteristics of the thruster system. Figures 2, 3 and 4 show the thruster board assembly, thruster in its box and mounted

**Table 1. PPT specifications**

Mass	210 g
Dimensions	90.17 x 95.89 x 31 mm
Impulse Bit	38.2 $\mu$ Ns
Total Impulse	42 Ns
Specific Impulse	608 s
Power	0.3-4W
Thrust to power ratio	20 $\mu$ N/W

within a cubesat structure, respectively.

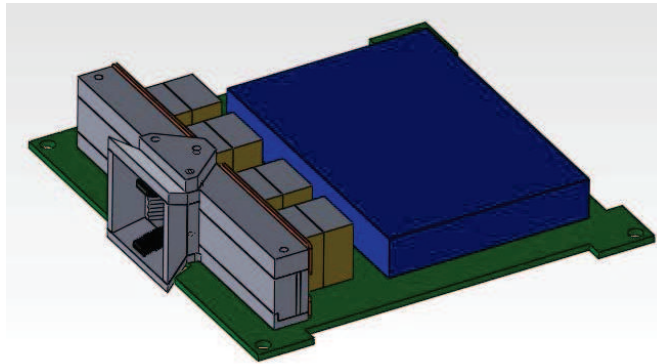


**Figure 2. PPTCUP-QM board, discharge chamber and electronics (blue box) assembly.**

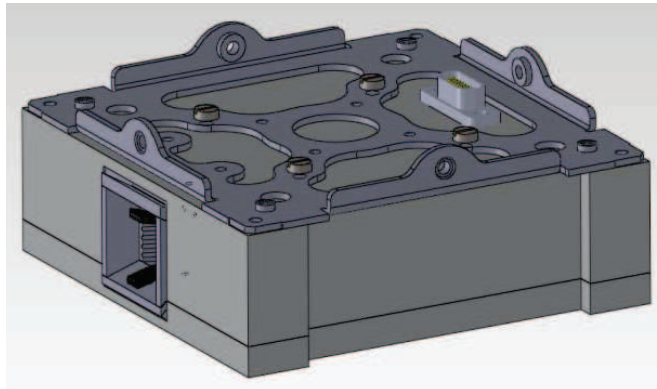


**Figure 3. Thruster in its box.**

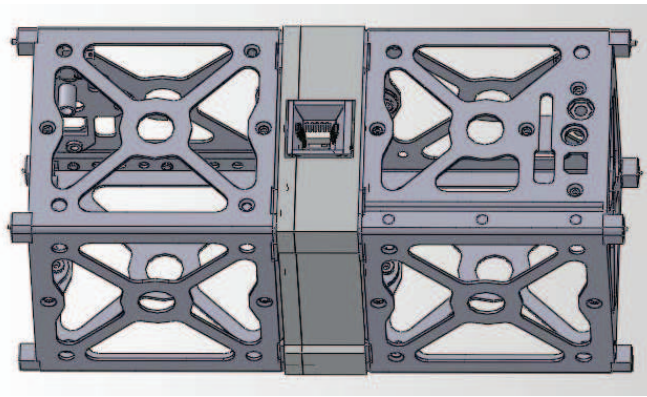


Figure 4. PPTCUP assembly within cubesat structure.

### III. Preliminary and expected results

Preliminary results for the application of Pulsed Plasma Thruster (PPT) technology have been obtained for a sample rendezvous and docking mission, accomplished by two small satellites flying in close formation at low altitudes. The objective of the reference mission is to perform rendezvous and docking of a leader-follower spacecraft pair. The leader satellite is passive, while the follower actively controls its relative position with respect to the leader to achieve the desired formation configuration. Both satellites are characterized by identical physical parameters. The total mass of each one is 3 kg. The bus size is 30X10x10 cm and the cross-sectional area is 10X10. The satellite shape can be well-approximated by a rectangular cuboid layout model. At the beginning of the operative phase, the satellites are flying in a near circular polar orbit. The orbit altitude is around 450 km, which corresponds to an orbital period of approximately 94 minutes. The considered formation is separated by a short distance in the along-track direction. The follower spacecraft is required to track the leader spacecraft and to dock it, using a set of two opposite PPT's per axis to control its position.

#### A. Formation flying control

The formation flying model state includes the leader position and velocity vectors ( $\mathbf{r}_L$ ,  $\mathbf{v}_L$ ), and the follower ones ( $\mathbf{r}_F$ ,  $\mathbf{v}_F$ ). The equations which describe evolution of the state vector in the ECI frame are:

$$\dot{\mathbf{r}}_L = \mathbf{v}_L \quad (1)$$

$$\dot{\mathbf{v}}_L = -\frac{\mu}{r_L^3} \mathbf{r}_L + \mathbf{a}_L \quad (2)$$

$$\dot{\mathbf{r}}_F = \mathbf{v}_F \quad (3)$$

$$\dot{\mathbf{v}}_F = -\frac{\mu}{r_F^3} \mathbf{r}_F + \mathbf{a}_F, \quad \mathbf{v}_F^+ = \mathbf{v}_F^- + \Delta \mathbf{v}_u \quad (4)$$

where  $\mu$  is the gravitational parameter of the Earth,  $\mathbf{a}_L$  and  $\mathbf{a}_F$  are the environmental perturbations and eq.(4) accounts for the impulsive change  $\Delta \mathbf{v}_u$  of the follower velocity due to PPT operation. The calculation of disturbance accelerations is based on the main orbital perturbations acting on spacecraft at low altitudes:

- Earth's non-spherical gravity field: A spherical harmonic expansion [EGM96] up to degree and order 9 is considered.
- Aerodynamic drag: The [Jacchia-71] model is employed to approximate the atmospheric density. The drag force acting on the satellite is calculated using a mean cross-sectional area.
- Solar radiation pressure: A Cannonball model is employed for the calculation of the solar radiation force, which takes into account eclipse conditions.

- Luni-solar attraction: Disturbance accelerations due to point-mass lunar and solar gravity field are considered. The position of the Sun and Moon is obtained through precise ephemerides.

A simple proportional-derivative (PD) control law is considered for formation flying control. In order to dock the leader, the follower spacecraft must drive its relative position and velocity to zero. Reference smoothing is not addressed in this work, so the tracking error can be expressed in a local coordinate frame (LVLH, see Fig. 5) as

$$\delta \mathbf{r} = \mathbf{R}_F^I (\mathbf{r}_L - \mathbf{r}_F) \quad (5)$$

$$\delta \mathbf{v} = \delta \dot{\mathbf{r}} = \mathbf{R}_F^I (\mathbf{v}_L - \mathbf{v}_F) + [\boldsymbol{\omega}_{LVLH} \times] \mathbf{R}_F^I (\mathbf{x}_L - \mathbf{x}_F) \quad (6)$$

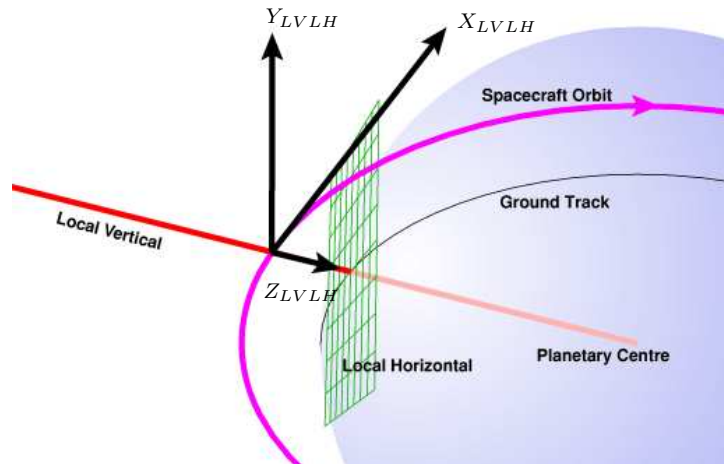


Figure 5. LVLH reference frame

where the coordinate transformation between the inertial frame and the local frame is expressed by the matrix  $\mathbf{R}_F^I$  and  $[\boldsymbol{\omega}_{LVLH} \times]$  is the skew-symmetric matrix of the LVLH rate  $\boldsymbol{\omega}_{LVLH}$ . The commanded thrust is calculated as

$$\mathbf{u} = \mathbf{K}_r \delta \mathbf{r} + \mathbf{K}_v \delta \mathbf{v} \quad (7)$$

where  $\mathbf{K}_r$  e  $\mathbf{K}_v$  are the gain matrices of the controller. The gain matrices have the following structure

$$\mathbf{K}_r = \begin{bmatrix} K_r & 0 & 0 \\ 0 & K_r & 0 \\ 0 & 0 & K_r \end{bmatrix} \quad \mathbf{K}_v = \begin{bmatrix} K_v & 0 & 0 \\ 0 & K_v & 0 \\ 0 & 0 & K_v \end{bmatrix} \quad (8)$$

An integral pulse frequency modulator is used to translate the continuous command signal into discrete pulses, as required for operation of PPT's. The modulator commands a pulse whenever the integral of the commanded thrust is greater or equal than the impulse bit  $\Delta u_M$  of the thrusters. Subsequently, the integral of the commanded thrust is set to zero to avoid integral wind-up. For each component  $u_i$  of the commanded thrust, we have that

$$\Delta u_i(t_k) = \Delta u_i(t_{k-1}) + \int_{t_{k-1}}^{t_k} u_i dt \quad (9)$$

where  $t_k - t_{k-1}$  is equal to the modulator step size. The modulator output is calculated as:

$$p_i(t_k) = \begin{cases} \Delta u_M \text{sgn}(\Delta u_i(t_k)) & \text{if } |\Delta u_i(t_k)| \geq \Delta u_M \\ 0 & \text{if } |\Delta u_i(t_k)| < \Delta u_M \end{cases} \quad (10)$$

If  $|\Delta u_i(t_k)| \geq \Delta u_M$ ,  $\Delta u_i(t_k)$  is set to zero for the calculation of  $\Delta u_i(t_{k+1})$ . The impulsive velocity change, expressed in the inertial frame, is given by

$$\Delta \mathbf{v}_u = \mathbf{R}_F^I \frac{\mathbf{p}}{m_F} \quad (11)$$

where  $m_F$  is the mass of the follower spacecraft,  $\mathbf{R}_F^I = (\mathbf{R}_F^I)^T$  and  $\mathbf{p} = [p_x, p_y, p_z]^T$ .

## B. Simulation results

A nonlinear simulation model has been developed, using MATLAB, for the considered formation flying scenario. The model includes the leader and follower perturbed translational dynamics as well as the control system of the follower spacecraft. The most relevant simulation parameters are reported in Table 2.

Altitude	450 km
Simulation time	5000 s
Proportional gain $K_r$	$7.5 \cdot 10^{-5}$
Derivative gain $K_v$	0.05
Modulator frequency	1 Hz
Impulse bit $\Delta u_M$	$40 \mu\text{Ns}$

**Table 2. Simulation parameters**

The proportional and derivative gains have been chosen through numerical simulations to obtain a system response with almost no position overshoot in the along-track direction.

At the beginning of the simulation, the formation is separated 12 m in the along-track direction. The follower spacecraft actively controls its position to dock the leader. The performance of the control system is reported in Figures 6 and 7, in terms of position and velocity tracking errors. It can be seen that the follower spacecraft succeeds in docking the leader, since both the relative position and velocity at the end of the simulation are near zero, for all axes. In particular, the final separation between the leader and the follower is just 3.5 mm. The control profile, reported in Fig. 8 for all axes, is compatible with the considered PPT technology.

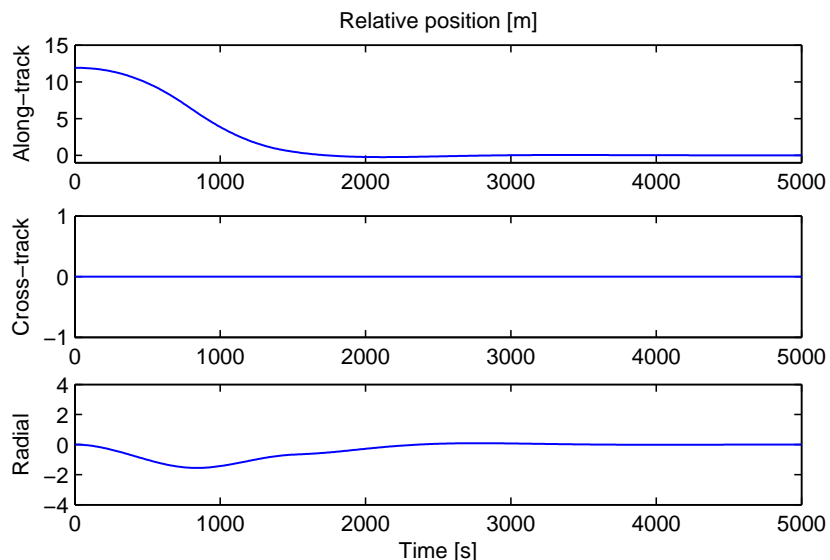


**Figure 6. Relative position tracking error.**

The applicability range of the Proportional plus Derivative Controller is limited by its structure but it provides a benchmark for comparison with other designs. In this application area, constrained control systems design is an obvious area for further investigation. One method that would enable constraints to be placed on inputs outputs and their rates of change is to use Model Predictive Control (MPC). Of the many algorithms available under this class of control algorithms, this work will first consider a design based on receding horizon control with a linearized model of the dynamics about an operating point.

Suppose that for some operating point, the linearized dynamics can be represented by the state-space

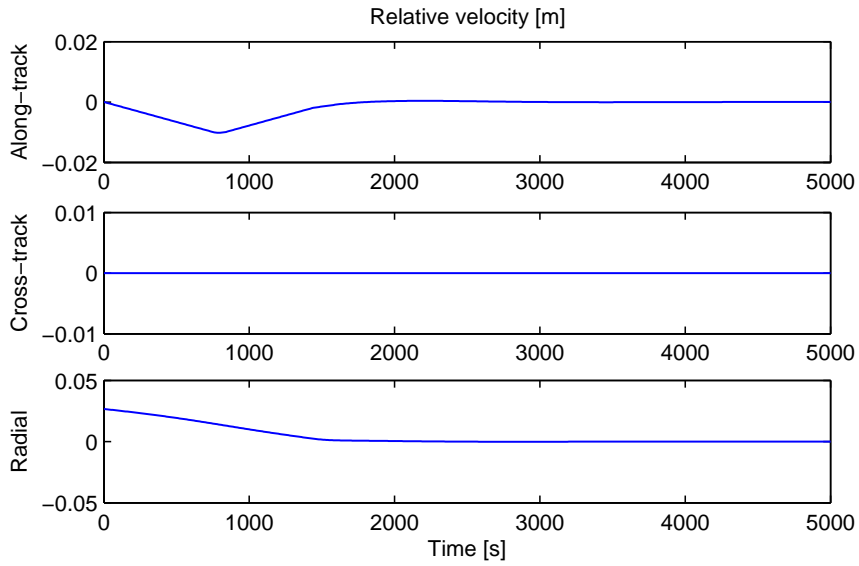


Figure 7. Relative velocity tracking error.

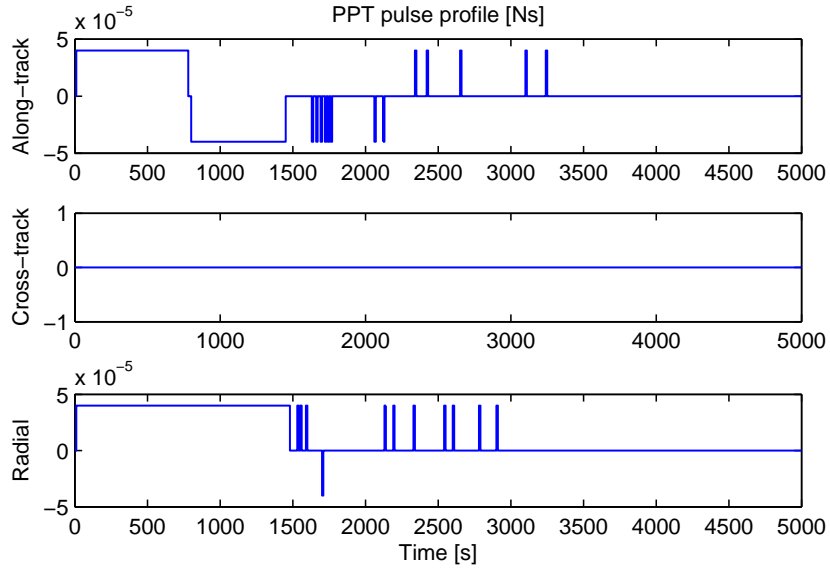


Figure 8. PPT impulse profile.

model

$$\begin{aligned}\dot{x}_m(t) &= A_m x_m(t) + B_m u(t) + \epsilon \\ y(t) &= C_m x_m(t)\end{aligned}\tag{12}$$

where  $x_m(t)$  is the state vector,  $u(t)$  is the input vector,  $y(t)$  the output vector,  $A_m$ ,  $B_m$  and  $C_m$  are matrices with constant entries and compatible dimensions, and  $\epsilon$  is a vector representing disturbances on the state dynamics.

This future research will consider discrete model based MPC and hence (12) is discretized with sampling period  $T_s$  using a zero-order hold, resulting in the discrete state-space model

$$\begin{aligned}x_m(k+1) &= A_d x_m(k) + B_d u(k) + d_\epsilon \\ y(k) &= C_d x_m(k)\end{aligned}\tag{13}$$

where

$$d_\epsilon = \int_0^{T_s} e^{A_m \tau} \epsilon d\tau, \quad A_d = e^{A_m T_s}, \quad B_d = \int_0^{T_s} e^{A_m \tau} B_m d\tau, \quad C_d = C_m$$

and  $d_\epsilon$  is assumed to have constant entries. The MPC design used in this paper is that used in [4], which gives references to the tools used, where experimental verification on a robotic system is also reported, and the following is a summary of the main steps, for an  $m$ -input,  $q$ -output,  $n$ -state model.

In common with a PI control scheme, an integrator is embedded in the MPC design, which is also used for the following purposes: i) elimination of the vector  $d_\epsilon$  in (13), or  $\epsilon$  in (12), which contains motor parameters that have a certain degree of uncertainty associated with them in applications, and ii) removal of the load disturbance torque which is assumed to be an unknown constant. This is the first step and once complete the MPC design is undertaken using the incremental model where the defining vectors are the differences between the state, input and output vectors, respectively, for any two successive sample instants. Therefore, when the operating conditions change it is only necessary to update the set-point signals to reflect this change and the other steady-state values for the state variables are not required. However, the parameters in the system matrices (13) depend on the operating conditions and if these undergo a drastic change, parameter updating may be required, resulting in a gain scheduled predictive controller.

Let  $\Delta x_m(k) = x_m(k) - x_m(k-1)$  and  $\Delta u(k) = u(k) - u(k-1)$  denote the incremental state and input vectors, respectively, computed from the corresponding vectors in (12). Then, since the vector  $d_\epsilon$  has constant entries, the state dynamics in the incremental model are described by

$$\Delta x_m(k+1) = A_d \Delta x_m(k) + B_d \Delta u(k) \quad (14)$$

Also

$$\begin{aligned} y(k+1) - y(k) &= C_d(x_m(k+1) - x_m(k)) = C_d \Delta x_m(k+1) \\ &= C_d A_d \Delta x_m(k) + C_d B_d \Delta u(k) \end{aligned}$$

or

$$y(k+1) = C_d A_d \Delta x_m(k) + y(k) + C_d B_d \Delta u(k) \quad (15)$$

and the augmented state-space model for design is

$$\begin{aligned} x(k+1) &= Ax(k) + B\Delta u(k) \\ y(k) &= Cx(k) \end{aligned} \quad (16)$$

where

$$x(k) = \begin{bmatrix} \Delta x_m(k) \\ y(k) \end{bmatrix}, \quad A = \begin{bmatrix} A_d & 0 \\ C_d A_d & I \end{bmatrix}, \quad B = \begin{bmatrix} B_d \\ C_d B_d \end{bmatrix}, \quad C = \begin{bmatrix} 0 & I \end{bmatrix}$$

and for the remainder of this paper  $0$  and  $I$ , respectively, denote the zero and identity matrices of compatible dimensions. One immediate advantage of this incremental description of the dynamics is that the constant vector  $d_\epsilon$  has been removed from the design.

The MPC design requires the predicted future outputs for a number of steps ahead, where these are generated from the state-space model at the current sampling instant. Let  $x(k+i|k)$ ,  $\Delta u(k+i|k)$  and  $y(k+i|k)$  denote the corresponding vectors in (16) at sample instant  $k+i$  given them at sample instant  $k$ . Then the state dynamics  $N_P$  sampling instants ahead of  $k$  are given by

$$\begin{cases} x(k+1|k) = Ax(k) + B\Delta u(k) \\ x(k+2|k) = A^2x(k) + AB\Delta u(k) + B\Delta u(k+1) \\ \vdots \\ x(k+N_p|k) = A^{N_p}x(k) + A^{N_p-1}B\Delta u(k) \\ \quad + \dots + A^{N_p-N_c}B\Delta u(k+N_c-1) \end{cases} \quad (17)$$

where  $N_p$  and  $N_c$  are termed the prediction and control horizons, respectively. Also the choice  $N_c \leq N_p$  assumes that the incremental control  $\Delta u$  has reached the steady-state after  $N_c$  instants, that is, after  $N_c$  samples the incremental control is assumed to be zero and  $N_c$  is a tuning parameter that decides the number



of future control inputs to be included in the optimization. The predicted output vectors for the next  $N_p$  instants can be written in the compact form:

$$Y = Fx(k) + \Phi\Delta U \quad (18)$$

where

$$\begin{aligned} Y &= \begin{bmatrix} y^T(k+1) & y^T(k+2) & \dots & y^T(k+N_p) \end{bmatrix}^T \\ \Delta U &= \begin{bmatrix} \Delta u^T(k) & \Delta u^T(k+1) & \dots & \Delta u^T(k+N_c-1) \end{bmatrix}^T \\ F &= \begin{bmatrix} (CA)^T & (CA^2)^T & \dots & (CA^{N_p})^T \end{bmatrix}^T \\ \Phi &= \begin{bmatrix} B & 0 & \dots & 0 \\ CAB & CB & \dots & 0 \\ \vdots & \vdots & \ddots & 0 \\ CA^{N_p-1}B & CA^{N_p-2}B & \dots & CA^{N_p-N_c}B \end{bmatrix} \end{aligned}$$

Let  $r(k)$  be the reference that is assumed to have constant entries within the prediction horizon and

introduce  $R_s = \bar{R}_s r(k) = \overbrace{\begin{bmatrix} I & I & \dots & I \end{bmatrix}^T}_{q \times N_p} r(k)$ . Then cost function used for the MPC design has the structure.

$$J = (R_s - Y)^T Q (R_s - Y) + \Delta U^T \bar{R} \Delta U \quad (19)$$

where  $Q$  is a  $(q \times N_p) \times (q \times N_p)$  symmetric positive semi-definite matrix and  $\bar{R}$  is a  $(m \times N_c) \times (m \times N_c)$  symmetric positive definite matrix. Of particular interest in the current application is the case when  $Q$  is a block diagonal matrix with diagonal block entries  $Q_{id}$  and  $Q_\omega$  and the structure

$$Q = \begin{bmatrix} Q_{id} & 0 & 0 & \dots & \dots & 0 \\ 0 & Q_\omega & 0 & \ddots & \dots & \vdots \\ 0 & 0 & \ddots & \ddots & \ddots & \vdots \\ \vdots & \ddots & \ddots & \ddots & \ddots & 0 \\ \vdots & \vdots & \ddots & \ddots & Q_{id} & 0 \\ 0 & \dots & \dots & 0 & 0 & Q_\omega \end{bmatrix}$$

and  $\bar{R}$  has the structure

$$\bar{R} = \begin{bmatrix} r_w & 0 & 0 & \dots & \dots & 0 \\ 0 & r_w & 0 & \ddots & \dots & \vdots \\ 0 & 0 & \ddots & \ddots & \ddots & \vdots \\ \vdots & \ddots & \ddots & \ddots & \ddots & 0 \\ \vdots & \vdots & \ddots & \ddots & r_w & 0 \\ 0 & \dots & \dots & 0 & 0 & r_w \end{bmatrix}$$

where  $r_w > 0$  is a scalar weighting. Note also that the structure of these weighting matrices is non-unique and application dependent. The choices given here are for illustrative purposes only.

Under the receding horizon principle, the control vectors for the next  $N_c$  sampling instants are obtained by minimizing the cost function (19) but only the first of these is applied to the plant. In the absence of constraints the global optimal solution is given by

$$\frac{\partial J}{\partial \Delta U} = 0$$

and solving this equation gives the global optimal control sequence as

$$\Delta U = (\Phi^T Q \Phi + \bar{R})^{-1} \Phi^T Q (\bar{R}_s r(k) - Fx(k))$$

Moreover, the control vector to be applied at the next sampling instant occurs when

$$\Delta u(k) = \begin{bmatrix} I & 0 & \dots & 0 \end{bmatrix} \Delta U$$

or

$$\Delta u(k) = K_y r(k) - K_x x(k) \quad (20)$$

where  $K_y$  is formed by the first  $m$  rows of  $(\Phi^T Q \Phi + \bar{R})^{-1} \Phi^T Q \bar{R}_s$  and  $K_x$  by the first  $m$  rows of  $(\Phi^T Q \Phi + \bar{R})^{-1} \Phi^T Q F$ .

The matrix  $\bar{R}_s$  forms the last  $q$  columns of the matrix  $F$  due to the special structure of the augmented state-space model matrices  $\mathbf{C}$  and  $\mathbf{A}$ . Consequently,  $K_y$  is given by the last  $q$  columns of the matrix  $K_x$  and, by using the relationship between  $K_x$  and  $K_y$ , the control law (20) can be written as

$$\begin{aligned} \Delta u(k) &= K_y r(k) - K_x \begin{bmatrix} \Delta x_m(k) \\ y(k) \end{bmatrix} \\ &= -K_x \begin{bmatrix} \Delta x_m(k) \\ y(k) - r(k) \end{bmatrix} \end{aligned} \quad (21)$$

Hence the control law to be applied is

$$u(k) = u(k-1) + \Delta u(k) \quad (22)$$

and in this constraints-free case,  $K_x$  can be computed off-line and  $u(k)$  computed online using (21) and (22).

Many different types of operational constraints often arise in the application of control algorithms to physical systems. In the case of a PMSM, the two input voltages to the motor,  $v_d$  and  $v_q$ , respectively, are limited by the d.c. bus voltage. Moreover, the maximum voltage that can be modulated by the Space Vector Pulse Width Modulator (SVPWM) is  $V_{dc}/\sqrt{3}$ . In the PI control structure, an anti-windup scheme is usually employed to compensate for constraints, but the success of MPC with constraints in, for example, process control applications makes it a natural alternative to be considered, particularly in the case of more than one input and output.

The cost function of the previous section was optimized with respect to  $\Delta U$ . Hence any constraints on, for example, the control inputs must first be translated into constraints on the incremental control vector  $\Delta u$ .

Consider first constraints on the amplitudes of the d and q-axis voltages and their incremental changes and let  $N_s (\leq N_c)$  denote the number of future sampling instants within the control horizon  $N_c$  where these are imposed. Then one form for them is

$$C_1(u_{min} - u(k-1)) \leq C_2 \Delta U \leq C_1(u_{max} - u(k-1)) \quad (23)$$

$$C_1 \Delta u_{min} \leq \Delta U \leq C_1 \Delta u_{max} \quad (24)$$

where  $C_1$  and  $C_2$  are matrices of dimensions  $(N_s \times m) \times m$  and  $(N_s \times m) \times (N_c \times m)$ , respectively, with the structure

$$C_1 = \begin{bmatrix} I & I & \dots & I \end{bmatrix}^T, \quad C_2 = \begin{bmatrix} I & 0 & \dots & 0 \\ I & I & \dots & 0 \\ \vdots & \vdots & \ddots & \vdots \\ I & I & \dots & I \end{bmatrix}$$

If all future control signals were constrained by choosing  $N_s = N_c$ , the computational load would increase and could become prohibitively expensive. Hence it is preferable in practical applications that the parameter  $N_s$  is treated as a tuning parameter depending on the sampling time of the micro-controller employed.

In the case of the q-axis current  $i_q(k)$  consider

$$i_q(k+1) = i_q(k) + \Delta i_q(k+1)$$

with

$$\Delta i_q(k+1) = \begin{bmatrix} 0 & 1 & 0 & 0 & 0 \end{bmatrix} (Ax(k) + B\Delta u(k))$$

where the system matrices  $A$  and  $B$  are from incremental system state-space model (16). The constraint on the next sample instant prediction of this current considered in this work takes the form

$$i_q^{min} \leq i_q(k) + \begin{bmatrix} 0 & 1 & 0 & 0 & 0 \end{bmatrix} (Ax(k) + B\Delta u(k)) \leq i_q^{max} \quad (25)$$

where  $i_q^{min}$  and  $i_q^{max}$  are the specified limits. Moreover,  $i_q(k)$  and  $x(k)$  are measured quantities and hence all terms in (25). Hence  $\Delta u(k)$  is formulated as linear inequality constraint in a similar manner to that on  $u(k)$ .

The constraints considered in this paper can be expressed in the compact form as

$$M\Delta U \leq \gamma \quad (26)$$

and the constrained optimization problem can be solved by Quadratic Programming, that is, minimize the cost function (19) subject to a set of linear inequality constraints of the form given above. One of the methods available is based on an on-line search of the active constraints using Hildreth's QP algorithm. This method uses Lagrange multipliers, in the form of a vector  $\lambda \geq 0$ , as the decision variables and the constrained optimization problem solved is

$$\min_{\lambda \geq 0} \left( \frac{1}{2} \lambda^T H \lambda + \lambda^T K + constant \right) \quad (27)$$

where  $H = M(\Phi^T Q \Phi + \bar{R})^{-1} M^T$  and  $K = \gamma + M(\Phi^T Q \Phi + \bar{R})^{-1} F$ . Once  $\lambda$  is obtained the optimal  $\Delta U$  vector is

$$\begin{aligned} \Delta U &= (\Phi^T Q \Phi + \bar{R})^{-1} \Phi^T Q (\bar{R}_{sr}(k) - Fx(k)) \\ &\quad - (\Phi^T Q \Phi + \bar{R})^{-1} M_{act}^T \lambda_{act} \end{aligned} \quad (28)$$

where  $M_{act}$  and  $\lambda_{act}$  denote the active linear constraint matrix and Lagrange multiplier vector, respectively, formed from  $M$  and  $\lambda$  in (26).

## IV. Conclusions

In this paper, the applicability of a propulsion system based on PPT to cubesat size spacecraft has been investigated for a sample formation flying mission. To this purpose, a recent development of the PPT architecture, which is close to be flight-qualified and fully compatible with spacecraft of limited sizes, has been adopted. Preliminary simulations of a benchmark Proportional Derivative control law demonstrate the feasibility of the proposed approach for rendez-vous and docking of spacecraft flying in close formation. It is worth remarking that, in the general case, the limitations dictated by the thruster technology should be taken into account in the design of the control law. In this respect, the formalism and theory to solve an MPC problem within a receding horizon formulation is provided. A detailed simulation of such control scheme is the subject of current research activities. Further investigations will also include attitude estimation and control.

## References

- [1] M. Kobilarov, S. Pellegrino, "Trajectory Planning for Cubesat Short Time-Scale Proximity Operations", accepted/to appear in AIAA Journal of Guidance, Control, and Dynamics, 2012.
- [2] M. Coletti, F. Guarducci, S. B. Gabriel "A microPPT for Cubesat application: "Design and preliminary experimental results", Acta Astronautica, Vol. 69, (2011), pp. 200-208.
- [3] R. Pongyithum, S. M. Veres, S. B. Gabriel and E. Rogers, "Universal adaptive control of satellite formation flying", International Journal of Control, Vol. 78, No. 1, 2005, pp. 45-52
- [4] L. Wang, C. T. Freeman, S. Chai and E. Rogers, "Predictive-repetitive Control with Constraints: from Design to Implementation". Journal of Process Control 23, 2013, 956-967. .
- [5] S. Ciaralli, M. Coletti, F. Guarducci and S. B. Gabriel, "PPTCUP lifetime test results", IEPC-2013-164.